SABER temperature observations in the summer polar mesosphere and lower thermosphere: Importance of accounting for the CO_2 ν_2 quanta V–V exchange

Alexander A. Kutepov,[1,2,3] Artem G. Feofilov,[1] Benjamin T. Marshall,[4] Larry L. Gordley,[4] W. Dean Pesnell,[5] Richard A. Goldberg,[5] and James M. Russell III[6]

Received 24 April 2006; revised 23 July 2006; accepted 26 September 2006; published 8 November 2006.

[1] The polar summer thermal structure, with its cold mesopause and steep temperature gradients, both below and above the mesopause, produces the largest non-LTE effects in the CO_2 ν_2 mode manifold states. In this paper we focus on validating the non-LTE model applied for operational temperature retrievals from the SABER 15 μm limb radiance observations for these extreme conditions. We demonstrate that accounting for the redistribution of ν_2 quanta among various CO_2 isotopes shifts the retrieved summer 2002 polar mesopause altitude upwards by 2 to 4 km. It brings the SABER temperature measurements into a better agreement with those of falling sphere experiments, lidar observations, as well as with climatological data.
Citation: Kutepov, A. A., A. G. Feofilov, B. T. Marshall, L. L. Gordley, W. D. Pesnell, R. A. Goldberg, and J. M. Russell III (2006), SABER temperature observations in the summer polar mesosphere and lower thermosphere: Importance of accounting for the CO_2 ν_2 quanta V–V exchange, *Geophys. Res. Lett.*, *33*, L21809, doi:10.1029/2006GL026591.

1. Introduction

[2] The SABER instrument on TIMED measures the limb radiance in ten broadband infrared channels over an altitude range that spans the mesosphere and lower thermosphere (MLT). Included are three 15 μm channels used for retrieving temperatures from the CO_2 limb emission. *Mertens et al.* [2004] demonstrated that accounting for the non-local thermodynamic equilibrium in the CO_2 is crucial for adequate retrieval of temperature in summer polar MLT. Nevertheless, the retrieved SABER temperatures differed significantly from those obtained from coincident falling sphere (FS) measurements taken during the 1–5 July 2002 summer MaCWAVE (for Mountain and Convective Waves Ascending Vertically) campaign [*Goldberg et al.*, 2004] at Andoya, Norway (69°N, 16°E). In particular it was noticed that the SABER mesopause was always lower in altitude (by up to 3 km) and colder compared to the FS measurements as well as to the climatological profiles presented by *Lübken* [1999] for early July. These discrepancies were deemed worthy of investigation due to mounting evidence that the SABER summer mesopause was too low in both altitude and temperature. That evidence also includes comparisons with lidar data [*She et al.*, 2002; *Goldberg et al.*, 2004; *Fritts et al.*, 2004]. Additionally, the SABER temperatures lead to NLC formation below 80 km in the CARMA model (M. Stevens, private communication, 2005). This is not supported by NLC observations [see *Fiedler et al.*, 2003].

[3] In this paper we focus on validating the SABER operational non-LTE model for polar summer conditions. We demonstrate that accounting for the redistribution of the ν_2 quanta among the first excited levels of various CO_2 isotopes significantly improves the agreement between temperatures retrieved from the SABER limb radiances and those from FS experiments and the climatological data.

2. Vibrational Temperatures of the CO_2 ν_2 Levels

[4] In the lower atmosphere inelastic molecular collisions determine the population of molecular levels. As a result local thermodynamic equilibrium (LTE) exists where the populations obey the Boltzmann law with the local kinetic temperature T_{kin}. In the middle and upper atmosphere the frequency of collisions is lower and other processes which populate and depopulate molecular levels (absorption and emission of radiation in molecular bands, redistribution of excitation between colliding molecules, chemical excitation) must be taken into account. In this region of the atmosphere LTE no longer applies and the populations of vibrational levels deviate from the Boltzmann distribution for the local T_{kin}. Such conditions are referred to as non-LTE and the populations n_v must be found by a self-consistent solving the system of rate equations expressing the balance of all processes which populate and depopulate vibrational levels v, and the radiative transfer equation in the ro-vibrational bands.

[5] The non-LTE population of molecular vibrational level is usually described by a vibrational temperature, T_v, which defines the excitation degree of level v against the ground level 0,

$$n_v/n_0 = g_v/g_0 \exp[-(E_v - E_0)/kT_v], \qquad (1)$$

in the Boltzmann formula applied to the ratio of the non-LTE populations. Here g_v and E_v are the statistical weight and the energy of level v, respectively. If $T_v = T_{kin}$ then level v is in LTE.

[1]Oak Ridge Affiliated Universities/NASA Goddard Space Flight Center, Greenbelt, Maryland, USA.
[2]Department of Physics, Catholic University of America, Washington, D. C., USA.
[3]University Observatory Munich, Faculty for Physics, Ludwig Maximilian University, Munich, Germany.
[4]GATS, Inc., Newport News, Virginia, USA.
[5]NASA Goddard Space Flight Center, Greenbelt, Maryland, USA.
[6]Center for Atmospheric Sciences, Hampton University, Hampton, Virginia, USA.

0094-8276/06/2006GL026591

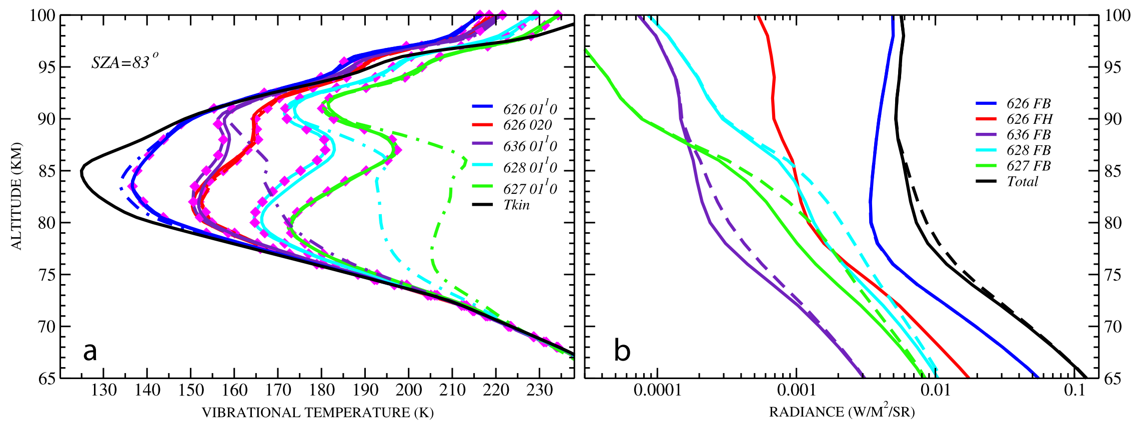

Figure 1. (a) Vibrational temperatures of CO_2 vibrational levels in the polar summer MLT. Solid lines: ALI-ARMS model, dashed-dotted lines: SABER operational model with the V–V exchange neglected, solid lines with diamonds: SABER operational model with V–V exchange implemented. (b) Simulated limb radiances in the SABER channel 1 (narrow 15 μm channel). Dashed lines: SABER operational model with the V–V exchange neglected, solid lines: SABER operational model with V–V exchange implemented.

[6] For the linear CO_2 molecule, v represents the combination of four indices $v_1 v_2^l v_3$ specifying the vibrational state, where v_1, v_2, and v_3 are the quantum numbers of symmetric stretching, bending and asymmetric stretching vibrational modes, respectively, and l is the vibrational angular momentum quantum number. Bands of four CO_2 isotopes $^{12}C^{16}O_2$[0.984], $^{13}C^{16}O_2$[1.1 $\times$ 10^{-2}], $^{16}O^{12}C^{18}O$[3.9 $\times$ 10^{-3})] and $^{16}O^{12}C^{17}O$[7.3 $\times$ 10^{-4}] (hereafter 626, 636, 628, and 627, respectively, where numbers in brackets give isotopic abundance), contribute to the limb radiance in the SABER 15 μm channels.

2.1. SABER Operational Non-LTE Model and ALI-ARMS Model

[7] The SABER non-LTE operational model [*Mertens et al.*, 2001] is based on the standard Curtis-matrix technique [*Goody*, 1964; *López-Puertas and Taylor*, 2001] for solving the non-LTE problem. It utilizes the "two level approach to the multilevel problem" where the populations n_v for each of four CO_2 isotopes are found by solving a sequence of the two-level problems starting from lower vibrational levels towards higher ones ($01^10 \rightarrow 020 \rightarrow 030$, etc.). Groups of closely spaced energy levels with equal ν_2 excitation are treated as single levels ([02^00, 02^20, 10^00] $\rightarrow$ 020, [03^10, 03^30, 11^10] $\rightarrow$ 030, etc.). This is an iterative algorithm: the populations of all other vibrational levels that enter the balance equation for the two selected levels are assumed to be known and updated by iterating the two-level problem sequence.

[8] We compared MLT vibrational temperatures of the CO_2 ν_2 manifold levels produced by the SABER operational non-LTE model with those from the ALI-ARMS (for Accelerated Lambda Iterations for Atmospheric Radiation and Molecular Spectra) non-LTE model. As inputs the SABER current V1.06 temperature, pressure, and VMRs of main atmospheric constituents, including those for CO_2 and O(^3P) were used. The ALI-ARMS model [see *Kutepov et al.*, 1998; *Gusev and Kutepov*, 2003, and references therein] directly solves the multi-level problem by means of the accelerated lambda iteration (ALI) technique developed in the 1990s in stellar astrophysics for calculating non-LTE populations of atomic and ionic levels. ALI is now the standard technique for computing non-LTE model stellar atmospheres and the observed spectra. The ALI-ARMS model was successfully applied by *Kaufmann et al.* [2002, 2003] and O. A. Gusev et al. (Atmospheric neutral temperature distribution at the mesopause/turbopause altitude, submitted to *Journal of Atmospheric and Solar-Terrestrial Physics*, 2006) to the non-LTE diagnostics of the spectral Earth's limb observations from CRISTA (Cryogenic Infrared Spectrometers and Telescopes for the Atmosphere) on the ASTRO-SPAS satellite [*Offermann et al.*, 1999; *Grossmann et al.*, 2002].

2.2. Importance of the ν_2 Quanta V–V Exchange in the Summer Polar MLT

[9] We found maximum differences in T_v from the two models of up to a few K in polar winter (~2 K), tropical (~6 K) and mid-latitude (~13 K) atmospheres in and around the mesopause for the level 01^10 of the weakest CO_2 isotope 627 included in the modeling. For more abundant isotopes and particularly for the 020 first hot (FH) and 030 second hot (SH) levels of the 626 isotope the differences were significantly smaller. For the summer polar MLT the situation was, however, quite different. One may see in Figure 1a very strong T_v differences between the two models for the 01^10 levels of all minor isotopes in the altitude region between 72 and 92 km. In this region T_v of minor isotopes provided by the ALI-ARMS model (solid lines) are significantly colder (up to 32 K for isotope 627) than those of the SABER code (dash-dotted lines). Additionally, the ALI-ARMS T_v for the 01^10 level of the main isotope is about 4 K warmer at the mesopause than that of SABER code, whereas the T_v for the level 020 of main isotope are in good agreement (the difference does not exceed 1.5 K).

[10] We determined that the T_v differences illustrated in Figure 1a were mainly caused by neglecting the collisional vibrational–vibrational (V–V) ν_2 quanta exchange between 01^10 levels of CO_2 isotopes

$$CO_2^i(01^10) + CO_2^j(0) \xrightarrow{V-V} CO_2^i(0) + CO_2^j(01^10) \qquad (2)$$

in the SABER operational model. In the summer polar atmosphere the upwelling radiation from the warm stratosphere is absorbed by CO_2 molecules of minor isotopes in

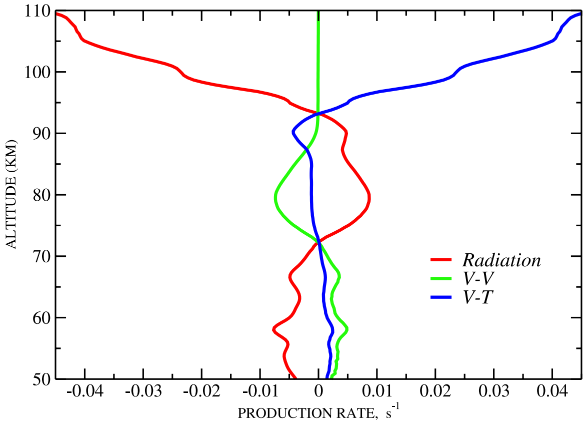

Figure 2. Net radiative and collisional production rates per molecule for the 01^10 level of isotope $^{13}C^{16}O_2$.

and around the very cold mesopause making, T_v of the 01^10 minor isotopic levels there significantly warmer than the kinetic temperature (see SABER dash-dotted curves in Figure 1a). This is, however, not true for the 01^10 level of main isotope 626: the fundamental 15 μm band of this isotope is optically thick — allowing the exchange of radiation only between near-by altitude levels and keeping this T_v much closer to the kinetic temperature. In this situation the collisional redistribution of the ν_2 quanta by V–V exchange plays a significant role: it tends to bring the ν_2 quanta levels in LTE. If the V–V exchange totally dominated all other processes it would lead to the equality of T_v for all levels involved. In the polar MLT, where other processes remain significant, the V–V exchange provides a strong shift of T_v for the 01^10 minor isotopic levels toward that of 626, demonstrating the loss of excitation in favor of the latter level (see Figure 1a). However, the 626 01^10 level contains about 98% of the ν_2 quanta reservoir, so its T_v exhibits only a minor increase. Figure 2 provides additional details of this redistribution process in the polar MLT. This figure shows the net radiative and collisional production rates for molecules of the isotope 636 in the vibrational state 01^10 that enter the rate equation for this state. One may see that, in the altitude range of 73–94 km, the absorption of radiation in the 636 15 μm fundamental band provides the main source of excitation of this level. This excitation is balanced by the thermalization of quanta due to the V–T transfer by collisions with N_2 and O_2 molecules and $O(^3P)$ atoms and by the V–V transfer of quanta to other CO_2 levels (mostly to the 626 01^10 level). The V–V transfer is the more efficient mechanism for removing the ν_2 quanta from the 636 01^10 level up to an altitude of 87.5 km. Above this altitude V–T transfer onto $O(^3P)$ starts dominating the quanta removal process.

[11] After the V–V exchange between CO_2 isotopes was implemented in the SABER non-LTE operational model we observed significant reductions of the differences between T_v of the models. For polar winter, tropical, and mid-latitude conditions the new differences did not exceed 1 K. In the summer polar atmosphere (see Figure 1a) SABER T_v of the 01^10 levels obtained with the V–V exchange implemented (solid lines with diamonds) exhibited a strong shift towards those of the ALI-ARMS model, the remaining differences do not exceed 1.5 K. They are most probably caused by the differing approaches to solving the radiative transfer equation in the codes, detailed discussion of which is beyond the scope of this work.

3. Simulated SABER Limb Radiances

[12] The T_v of the SABER model were next used as inputs to the BANDPAK code [*Marshall et al.*, 1994] and the total limb radiances in SABER channel 1 (narrow 15 μm channel) as well as the contributions of different bands to this signal were calculated. The total signal and its main components are presented in Figure 1b. One may see in Figure 1b that, in and around the mesopause, the total contribution of the fundamental bands of minor CO_2 isotopes to the signal is comparable to that of the fundamental band of the main isotope. Additionally, these bands are strongly affected by the T_v differences discussed above. As a result the signal calculated for the SABER T_v when the ν_2 quanta V–V exchange between the first excited levels of all isotopes is neglected differs in the 70–90 km altitude region from the signal obtained with the implemented V–V exchange. Below the altitude of 90 km the new signal is significantly lower, the maximum relative difference $(I_{total}^{no\ V-V} - I_{total})/I_{total}$ reaches the value of 17% at the altitude of 80 km. As was discussed above, turning on the ν_2 quanta V–V exchange leads to significant decreases in the T_v of the 01^10 minor isotopic levels below and around the mesopause and a relatively small increase of the 626 01^10 level T_v (see Figure 1a). The latter, however, does not compensate the fall of total radiance caused by the corresponding decrease of the radiances in the minor isotopic fundamental bands.

4. Improved Temperature Retrievals in Summer Polar MLT

[13] With the modified SABER non-LTE model we retrieved temperatures in the summer polar MLT. In Figure 3 we compare these retrievals for a typical single scan of the summer polar MLT (July 2, 2002, orbit 03055, event 19, time 00:32:08, latitude = 72.13°N, longitude = 18.96°E) with that obtained from the unmodified model, as well as with the temperature profile obtained in a nearly coincidental FS experiment (July 2, 2002, flight MMVFS09, latitude = 69.30°N, longitude = 16.02°E), and the climatological profile of *Lübken* [1999] for early July. One can see

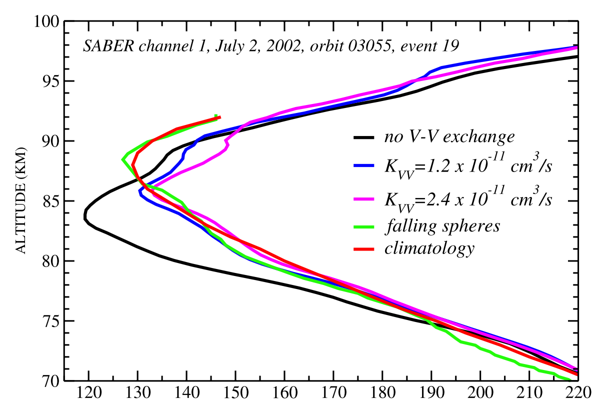

Figure 3. Temperature retrievals in polar summer MLT, SABER channel 1 (narrow 15 μm channel).

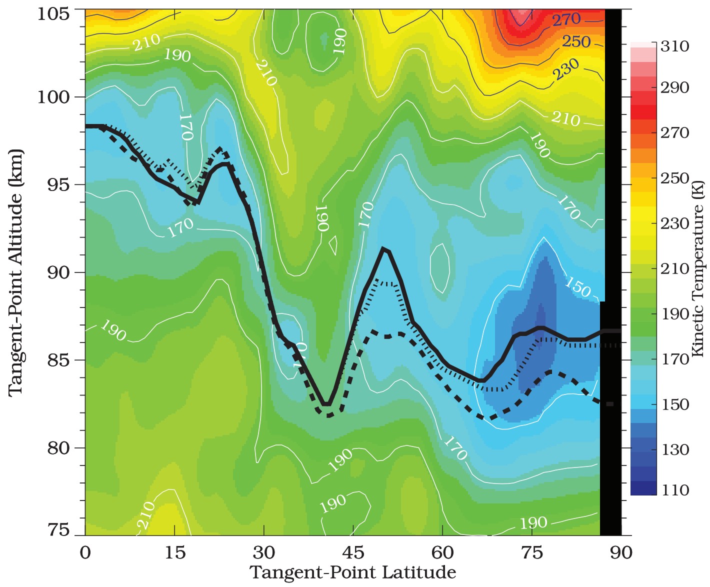

Figure 4. Temperatures retrieved for events 25–51, orbit 3094, July 4, 2002. Black lines give mesopause altitude: solid - this study, dotted - twice lower V–V exchange rate, dashed - current V1.06 temperature product, no V–V exchange.

in Figure 3 that the new temperature profile is warmer than the old one in the altitude region of 75–90 km. This warming results from the decreased T_v of the CO_2 01^10 minor isotopic levels in the same altitude region (see Figure 1a). The corresponding drop of calculated radiances (see Figure 1b) requires higher kinetic temperatures in order to fit the measured signal. Finally, concomitant changes in hydrostatic equilibrium in the iterative temperature fitting due to this warming result in a total 2–2.5 km shift of the mesopause to an altitude of about 85–86 km compared to that of the old profile located at the altitude 83–84 km.

[14] The results presented in Figure 3 were obtained using the rate coefficient for quenching $CO_2(\nu_2)$ by collisions with $O(^3P)$ atoms $K_O = 6 \times 10^{-12}$ cm^3 s^{-1} (for $T = 300$ K) and for the CO_2 VMR profile from the SABER current V1.06 data product, which keeps constant till the altitude of 80 km. The application of $K_O = 1.5 \times 10^{-12}$ cm^3 s^{-1} (which is equivalent to applying the four time lower $[O(^3P)]$) has insignificant impact on the retrieved temperatures below 80 km, gives 10 K warmer mesopause, keeps, however, mesopause at the same altitude, and leads to lower temperatures above 90 km (by 25 and 40 K at the altitudes of 95 and 100 km, respectively). Increasing/decreasing the altitude to which CO_2 VMR keeps its constant value by 5 km also has no effect on retrievals below 80 km, shifts, however, the mesopause altitude and temperature by ±0.5 km and ±2 K, respectively, and decreases/increases temperature above 86 km (by 10 K at 100 km).

5. Value of the ν_2 V–V Rate Coefficient

[15] The value of the rate coefficient $k_{\nu_2}^{V-V} = 1.2 \times 10^{-11}$ cm^3 s^{-1} applied for the process (2) in the calculations described above was recommended by *López-Puertas and Taylor* [2001, p. 170, Table 6.2]. *Huddleston and Weitz* [1981] obtained this value by measuring the total quenching rate coefficient of the process

$$CO_2(020) + CO_2(0) \xrightarrow{V-V} 2CO_2(01^10) \tag{3}$$

for the main isotope, where 020 denotes three closely spaced energy levels considered as a combined single level. This value has been adopted in many studies (see, for example references in *López-Puertas and Taylor* [2001]) including the SABER non-LTE model as the rate coefficient for both processes (2) and (3) as well as for processes of the type (3) with higher upper levels. In a later experiment the individual rate coefficients for each of three upper levels in reaction (3) were analyzed [*Dang et al.*, 1983]. It was found that the rate coefficient for the level 02^20 was about four times higher than that for the entire triad as well as significantly higher than those for the other two levels. This result was supported by the quantum-mechanical analysis by *Orr and Smith* [1987]. Scaling the value of *Dang et al.* [1983] for the 02^20 level by means of the rule which links rates of collisionally induced transitions to the quantum momenta squared of the corresponding radiative transitions, *Shved et al.* [1998] suggested a formula for any one-ν_2 quantum V–V exchange rate coefficient. If LTE is assumed within the 020 triad this formula gives nearly the same total rate coefficient of process (3) as that by *López-Puertas and Taylor* [2001]. However, the coefficient in reaction (2) is doubled.

[16] Doubling the rate coefficient for processes (2) in the SABER model drives the T_v of the minor CO_2 isotopes even closer to that of the main isotope (up to 11, 9, and 6 K for isotopes 627, 628, and 636, respectively). This leads to an additional drop of the calculated radiance in the mesosphere by up to 10% and, therefore, to an increase in T_{kin} retrieved in the altitude range 77–91 km (Figure 3).

6. Impact of Using the Modified Non-LTE Model in the Operational SABER Processing Code

[17] We evaluated the impact of using the modified SABER non-LTE model in the operational SABER processing code. We used a set of events (events 25–51, orbit 3094, July 4, 2002) employed in the comparison of SABER to FS measurements in the first MaCWAVE campaign [*Mertens et al.*, 2004]. Figure 4 shows temperatures in the

MLT (as a color contour) retrieved using the modified SABER model plus a rate coefficient more consistent with the value in the ALI-ARMS code (2.4×10^{-11} cm^3 s^{-1}). The thick black solid line gives the corresponding mesopause altitude. The black dashed line and the black dotted line give the mesopause altitude for the current SABER V1.06 temperature product (where the ν_2 quanta V–V exchange was neglected) and for retrievals obtained using the modified SABER T_v code and $k_{\nu_2}^{V-V} = 1.2 \times 10^{-11}$ cm^3 s^{-1}, respectively. The primary impact of turning on the ν_2 quanta V–V exchange is a warming of the polar mesopause region and an upward shifting of the polar mesopause altitude by 2 to 3 km. The impact of doubling the $k_{\nu_2}{}^{V-V}$ rate constant is a further warming of the polar summer mesopause region. Additionally, the mesopause shifts upward another 0.5–1.0 km.

7. Conclusion

[18] We have demonstrated the importance of accounting for the ν_2 quanta V–V exchange between CO_2 isotopes for modeling the broadband 15 μm limb radiances. The accounting for the ν_2 quanta exchange between first excited levels of isotopes when retrieving temperatures in the polar summer MLT from the broadband 15 μm limb radiances measured by the TIMED/SABER instrument during the polar summer 2002 shifts the mesopause altitude upwards by 2 to 4 km. It brings these temperature measurements into a better agreement with the results of other observations, such as falling sphere experiments (see Figure 3), lidar observations [*She et al.*, 2002; *Goldberg et al.*, 2004; *Fritts et al.*, 2004], as well as with climatological data. Similar shifts of mesopause altitude were also observed in test retrievals for polar summers 2003–2005.

[19] The study also shows the impact of utilizing the higher value of *Shved et al.* [1998] for the rate coefficient of the ν_2 quanta V–V exchange between first excited levels of CO_2 isotopes.

[20] The implementation of the V–V exchange did, however, not solve entirely the disagreement problem: the altitude of mesopause remains still about 2 km lower than that of climatological and FS data (see Figure 3). New temperatures are also appreciably warmer above 86 km than the climatological and FS data. Additionally, below 75 km they do not reproduce the colder lower mesosphere obtained in the FS experiments during the MaCWAVE campaign.

[21] **Acknowledgments.** We wish to thank Peter Wintersteiner and other members of the SABER Algorithm team for their consideration and helpful comments. One of us (B.T.M.) was supported, in part, by a grant from NASA's SEC GI program.

References

Dang, C., J. Reid, and B. K. Garside (1983), Dynamics of the CO_2 upper laser level as measured with a tunable diode laser, *Appl. Phys. B*, *31*, 163–172.

Fiedler, J., G. Baumgarten, and G. von Cossart (2003), Noctilucent clouds above ALOMAR between 1997 and 2001: Occurrence and properties, *J. Geophys. Res.*, *108*(D8), 8453, doi:10.1029/2002JD002419.

Fritts, D. C., B. P. Williams, C. Y. She, J. D. Vance, M. Rapp, F.-J. Lübken, A. Müllemann, F. J. Schmidlin, and R. A. Goldberg (2004), Observations of extreme temperature and wind gradients near the summer mesopause during the MaCWAVE/MIDAS rocket campaign, *Geophys. Res. Lett.*, *31*, L24S06, doi:10.1029/2003GL019389.

Goldberg, R. A., et al. (2004), The MaCWAVE/MIDAS rocket and ground-based measurements of polar summer dynamics: Overview and mean state structure, *Geophys. Res. Lett.*, *31*, L24S02, doi:10.1029/2004GL019411.

Goody, R. M. (1964), *Atmospheric Radiation: Theoretical Basis*, Oxford Univ. Press, New York.

Grossmann, K. U., D. Offermann, O. Gusev, J. Oberheide, M. Riese, and R. Spang (2002), The CRISTA-2 mission, *J. Geophys. Res.*, *107*(D23), 8173, doi:10.1029/2001JD000667.

Gusev, O. A., and A. A. Kutepov (2003), Non-LTE gas in planetary atmospheres, in *Stellar Atmosphere Modeling: Proceedings of an International Workshop Held in Tübingen, Germany, 8–12 April 2002*, *Astron. Soc. Pac. Conf. Ser.*, vol. 288, edited by I. Hubeny, D. Mihalas, and K. Werner, pp. 318–330, Astron. Soc. of the Pac., San Francisco, Calif.

Huddleston, R. K., and E. Weitz (1981), A laser-induced fluorescence study of energy transfer between the symmetric stretching and bending modes of CO_2, *Chem. Phys. Lett.*, *83*, 174–179.

Kaufmann, M., O. A. Gusev, K. U. Grossmann, R. G. Roble, M. E. Hagan, C. Hartsough, and A. A. Kutepov (2002), The vertical and horizontal distribution of CO_2 densities in the upper mesosphere and lower thermosphere as measured by CRISTA, *J. Geophys. Res.*, *107*(D23), 8182, doi:10.1029/2001JD000704.

Kaufmann, M., O. A. Gusev, K. U. Grossmann, F. J. Martn-Torres, D. R. Marsh, and A. A. Kutepov (2003), Satellite observations of daytime and nighttime ozone in the mesosphere and lower thermosphere, *J. Geophys. Res.*, *108*(D9), 4272, doi:10.1029/2002JD002800.

Kutepov, A. A., O. A. Gusev, and V. P. Ogibalov (1998), Solution of the non-LTE problem for molecular gas in planetary atmospheres: Superiority of accelerated lambda iteration, *J. Quant. Spectrosc. Radiat. Transfer*, *60*, 199–220.

López-Puertas, M., and F. W. Taylor (2001), *Non–LTE Radiative Transfer in the Atmosphere*, World Sci., Hackensack, N. J.

Lübken, F.-J. (1999), Thermal structure of the Arctic summer mesosphere, *J. Geophys. Res.*, *104*, 9135–9149.

Marshall, B. T., L. L. Gordley, and D. A. Chu (1994), Bandpak: Algorithms for modeling broadband transmission and radiance, *J. Quant. Spectrosc. Radiat. Transfer*, *52*, 581–599.

Mertens, C. J., M. G. Mlynczak, M. López-Puertas, P. P. Wintersteiner, R. H. Picard, J. R. Winick, L. L. Gordley, and J. M. Russell III (2001), Retrieval of mesospheric and lower thermospheric kinetic temperature from measurements of CO_2 15 μm Earth limb emission under non-LTE conditions, *Geophys. Res. Lett.*, *28*(7), 1391–1394.

Mertens, C. J., et al. (2004), SABER observations of mesospheric temperatures and comparisons with falling sphere measurements taken during the 2002 summer MaCWAVE campaign, *Geophys. Res. Lett.*, *31*, L03105, doi:10.1029/2003GL018605.

Offermann, D., K.-U. Grossmann, P. Barthol, P. Knieling, M. Riese, and R. Trant (1999), Cryogenic Infrared Spectrometers and Telescopes for the Atmosphere (CRISTA) experiment and middle atmosphere variability, *J. Geophys. Res.*, *104*, 16,311–16,325.

Orr, J. B., and I. W. M. Smith (1987), Collision-induced vibrational energy transfer in small polyatomic molecules, *J. Phys. Chem.*, *91*, 6106–6119.

She, C. Y., J. D. Vance, B. P. Williams, D. A. Krueger, H. Moosmüller, D. Gibson-Wilde, and D. Fritts (2002), Lidar studies of atmospheric dynamics near polar mesopause, *Eos Trans. AGU*, *83*(27), 289, 292–293.

Shved, G. M., A. A. Kutepov, and V. P. Ogibalov (1998), Non-local thermodynamic equilibrium in CO_2 in the middle atmosphere. I. Input data and populations of the ν_3 mode manifold states, *J. Atmos. Sol. Terr. Phys.*, *60*, 289–314.

A. G. Feofilov and A. A. Kutepov, ORAU/NASA GSFC, Mail Code 693, Greenbelt, MD 20771, USA. (aak@usm.uni-muenchen.de)

R. A. Goldberg and W. D. Pesnell, NASA GSFC, Code 612.3, Greenbelt, MD 20771, USA.

L. L. Gordley and B. T. Marshall, GATS, Inc., 11864 Canon Blvd, Suite 101, Newport News, VA 23606, USA.

J. M. Russell III, Center for Atmospheric Sciences, Hampton University, P.O. Box 6075, Hampton, VA 23668, USA.